Temperature-dependent growth and structure of Cr deposited on Co(0001)

F. Scheurer, P. Ohresser, H. Bulou, J. P. Deville, and B. Carrière
Institut de Physique et Chimie des Matériaux de Strasbourg, UMR 046, 23 rue du Loess, F-67037 Strasbourg Cedex, France

A. Dobroiu
Institutul de Fizica Atomica IFTAR-Laseri, P.O. Box MG 36, 76900 Bucuresti Magurele, Romania
(Received 20 September 1996)

The growth and structure of ultrathin Cr films deposited on a Co(0001) single crystal are investigated for substrate temperatures ranging from 300 to 500 K by means of Auger electron spectroscopy, low-energy electron diffraction, and photoemission. Below 410 K, the interface is sharp and the Cr layers are in a Nishiyama-Wassermann-type epitaxy. Above 410 K, Cr grows pseudomorphically up to about one monolayer and then the structure turns to a Kurdjumov-Sachs orientation. For a growth temperature below 440 K uniaxial disorder appears when increasing the film thickness. [S0163-1829(97)06744-1]

I. INTRODUCTION

Cobalt-chromium multilayers have been extensively studied in several crystallographic orientations first because of their magnetic anisotropy and magnetoresistance properties, and second because of the possibility of stabilizing crystallographic phases.[1–4] Since the magnetic properties of multilayers are strongly dependent on the sharpness of the interface, the growth mode, and the crystallographic structure, it is interesting to compare systems built on various types of substrates and to determine their respective magnetic properties. Slightly different substrates can lead to very different growth modes or structures. For example, in molecular-beam-epitaxy– (MBE-) Co-Cr multilayers on mica and GaAs substrates giving hexagonal Co layers, it has been shown that a structural transition occurs between 2 and 6 Å from a pseudomorphic growth of Cr towards both Nishiyama-Wassermann and Kurdjumov-Sachs orientations.[3,4] On the other hand, pseudomorphic Cr layers have been observed up to nearly 18 Å on thick Co layers deposited on W(110).[5]

In this paper we analyze the growth of ultrathin Cr films deposited directly on a Co(0001) single crystal at temperatures between 300 and 500 K. The growth mode and the structure of the interface are investigated by means of Auger electron spectroscopy (AES), low-energy electron diffraction (LEED), and x-ray-photoemission spectroscopy (XPS).

II. EXPERIMENT

The growth and the structural studies were performed in an ultrahigh vacuum chamber (pressure in the low 10^{-10} mb range) equipped with a MAC2 Riber Auger analyzer and an Omicron reverse-view LEED optics. The Auger spectra were monitored continuously during the Cr evaporation. Additional XPS studies were performed in another chamber, equipped with a monochromatized Al x-ray source and a hemispherical analyzer. Temperatures were measured with a thermocouple pinned near the sample.

The Co single crystal was cleaned by argon-ion sputtering while annealing at 600 K and finally annealed at 650 K, to be sure to avoid the martensitic transition of Co. A carbon- and oxygen-free, well-ordered substrate can be obtained after several cycles. The Cr was evaporated from a tungsten basket containing high-purity polycrystalline chromium. The cleanliness of the substrate and Cr films was checked by AES or XPS. Several hours of outgassing were necessary to get carbide-free Cr layers. The thickness calibration was done by measuring the attenuation of the Auger *LMM* transition on the films grown at room temperature as described in Ref. 6 since these films show perfect exponential-shaped growth kinetics. The evaporation rate is estimated to about 0.10 ± 0.03 Å/min. The inelastic mean free path chosen is 9 Å for the *LMM* transitions, compatible with Ref. 7.

More than ten samples were grown for various substrate temperatures in the 300–500-K range. Between 370 and 440 K, several samples were repeatedly grown in steps of about maximum 10 K.

III. RESULTS

Figure 1 shows several Auger growth kinetics recorded for various substrate temperatures between 300 and 470 K. Two main growth regimes are observed: below 410 K [Figs. 1(a) and 1(b)], the growth kinetics are exponentially shaped and upon increasing temperature, they deviate more and more from the exponential shape [Figs. 1(c) and 1(d)].

A. Growth between 300 and 410 K

Up to 410 K [Figs. 1(a) and 1(b)], the intensity of the Co substrate Auger *LMM* transition decays exponentially with the deposited Cr amount and is nearly zero after about 30 Å Cr deposition (one monolayer having a thickness of approximately 2 Å). The Cr Auger transition intensity increases conversely. Such exponentially shaped growth kinetics are characteristic of a sharp interface and a simultaneous layer growth mode, i.e., a mode where new layers start growing while the previous ones are not completed.[8,9] No clear breaks, typical of a layer-by-layer growth, are observed in this temperature range. However, even at 370 K, the experi-

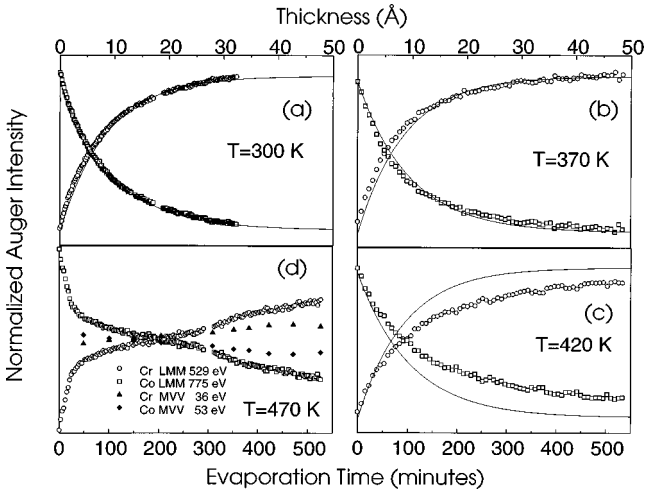

FIG. 1. Cr and Co Auger transition intensities as a function of the evaporation time at (a) 300 K, (b) 370 K, (c) 420 K, and (d) 470 K. Full lines: simulated growth kinetics for a simultaneous layer growth mode.

mental curves already start to deviate slightly from the calculated ones. A limited interdiffusion is thus probably already starting.

The LEED patterns show well-defined additional spots around the main substrate spots, from submonolayer coverage up to at least 12 Å [Fig. 2(a)]. This pattern is typically obtained for a bcc Cr(110) planar epitaxy on the Co(0001) surface in one of the two possible Nishiyama-Wassermann orientations (NW_x) as demonstrated in Fig. 2(b). The simulated NW_x pattern [Fig. 2(b)] results from the superimposition of three equivalent bcc (110) domains: for one domain, the bcc [001] direction is parallel to the dense [10$\bar{1}$0] substrate row, or equivalently, the bcc [110] direction is parallel to the hexagonal [12$\bar{3}$0] direction [Fig. 2(c)]. The two other domains are deduced by a $\pm 60°$ rotation of the previous one. Actually, three satellite spots should be observed in the LEED patterns for low coverage in the vicinity of a Co spot. In the case of Cr on Co(0001), however, the third spot is hidden by the main substrate spot. This means that the Cr lattice parameter is expanded by about 6% in the bcc [110] direction, whereas it remains unchanged in the [001] direction. Notice that in Fig. 2(c) the common origin of the Cr and Co lattices is chosen arbitrarily at the intersection of the [110] and [001] bcc directions. Due to the 6% expansion of the bcc lattice along [110], there is perfect matching in this direction, leading to the coincidence of the Co and Cr lattice points (dark and gray circles) along the dashed [110] direction and leading also to the typical alignment of the NW_x epitaxy in the perpendicular direction (but no coincidence since there is no distortion of the Cr lattice along [001]).

On further Co deposition, the LEED spots become progressively more elongated and the background gets brighter as can be seen in Fig. 2(d). A careful look at the inner spots shows tiny dark lines connecting the streaky spots together to form a hexagon.

$I(V)$ LEED curves (not shown here) of the specular LEED reflection indicate a very slight increase of the interlayer spacing for the thinner Cr films with respect to the

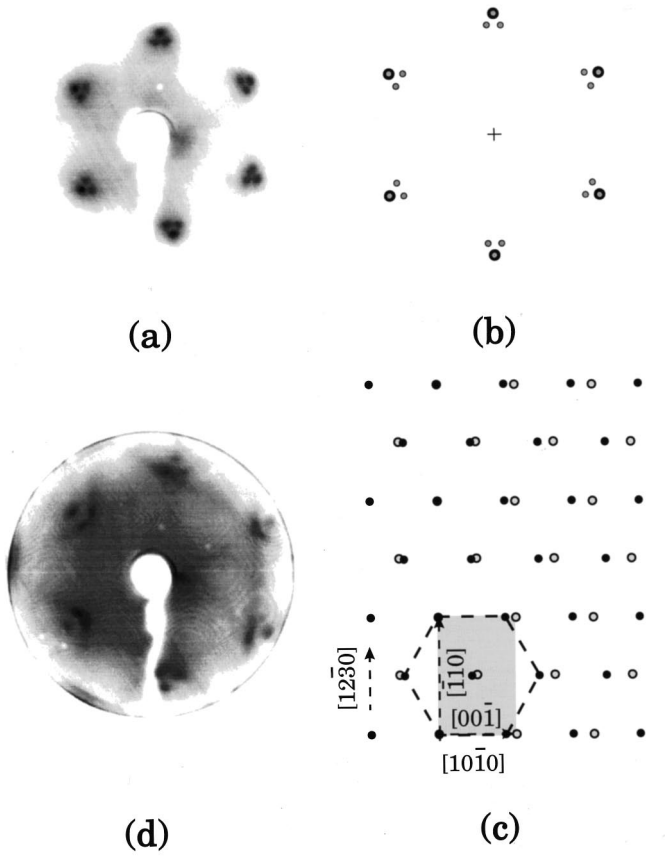

FIG. 2. (a) LEED pattern of a 6-Å Cr layer grown at 300 K (energy 119 eV); (b) simulation of the NW_x orientation (6% strained Cr layer in the [110] direction); black circles: Co spots; gray circles: Cr spots. (c) Real-space lattice of Co (black circles) and Cr (gray circles) for one Cr domain in the NW_x orientation (6% strained Cr layer in the [110] direction); (d) LEED pattern for a thick Cr film grown at 370 K (energy 100 eV) (see also text).

thicker ones. The expansion is estimated to less than 1.5%, though a simple kinematical approach cannot give a more precise value.

B. Growth between 410 and 470 K

The growth kinetics recorded for deposition on a substrate held at 420 K [Fig. 1(c)] deviate significantly from the exponential law of the simultaneous layer growth mode. The change is even more drastic at 470 K [Fig. 1(d)]. In this latter case, we clearly see that after about 2 Å coverage the intensity of the *LMM* Co (Cr) Auger transition decreases (increases) much more slowly. Since the growth is definitely not layer by layer, nor simultaneous, the thickness no longer corresponds to the true film thickness but must be understood as an equivalent thickness, i.e., as the amount of Cr that would be deposited to obtain the same thickness in the case of a layer-by-layer growth mode. Even for a 50-Å equivalent thickness, the low-energy Auger *MVV* transitions of Co are still visible [Fig. 1(d)]. The growth mode thus evolves progressively from a simultaneous layer growth mode below 410 K, to either a Stranski-Krastanov growth, or implies a diffuse interface formation.

Together with the growth mode, the structure observed by LEED also changes. There is an abrupt structural transition

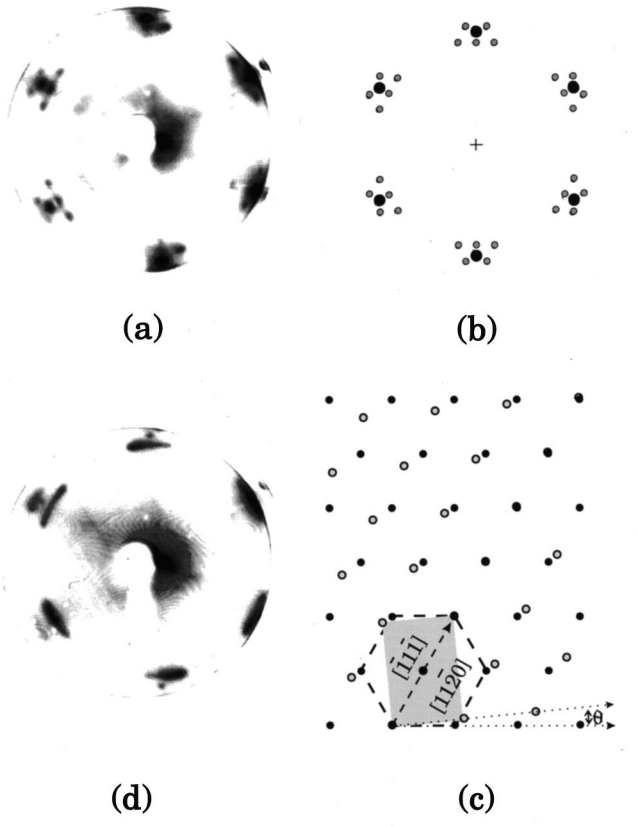

FIG. 3. (a) LEED pattern of a thick Cr layer grown at 470 K (energy 70 eV); (b) simulation of the KS orientation (1% strained Cr layer in the [110] direction); black circles: Co spots; gray circles: Cr spots. (c) Real-space lattice of Co (black circles) and Cr (gray circles) for one Cr domain in the KS orientation (1% strained Cr layer in the [110] direction); (d) LEED pattern for a thick Cr film grown at 420 K (energy 70 eV) (see also text).

around 410 K in a temperature interval less than 10 K. Below this temperature, the LEED pattern always shows the NW oriented layers, independently of the Cr thickness. For temperatures above 410 K, we observe a thickness dependence of the LEED pattern. A (1×1) LEED pattern is observed up to 2 or 3 Å, indicating a pseudomorphic growth. For thicker films, the LEED pattern changes and is typical of a Kurdjumov-Sachs (KS) orientation as can be seen in Fig. 3(a). The simulated pattern [Fig. 3(b)] is obtained by the superimposition of six bcc (110) domains on a hexagonal surface. For one domain, the [111] direction of the adsorbate is parallel to the [1120] substrate direction [Fig. 3(c)]. This type of orientation corresponds to a dense row matching, and therefore the bcc cell is rotated, compared to the NW case: the bcc [001] and hcp [1010] directions make an angle θ of 5.26°. The five other domains are deduced from the former one by applying a mirror symmetry [the symmetry plane being the hexagonal (1100) plane or the bcc (112) plane] and a ±60° rotation. In Figs. 3(a) and 3(b) one can see five satellite spots, all well separated from the main substrate spot. Actually, there are six satellites: the inner central satellite is composed of two perfectly superimposed spots occurring from two mirror domains. A precise image analysis indeed shows that the resulting spot is brighter than the other satellite spots. There may be a slight expansion of the lattice parameter, less than 1% along the bcc [$\bar{1}$10] axis, though this value is at the limit of what can be measured here.

For growth temperatures above 440 K, the LEED pattern still switches from the 1×1 to the KS pattern at a thickness of 3 Å, but then it does not evolve any more upon increasing thicknesses. The substrate spots are still visible at the highest coverage analyzed (50 Å equivalent deposition). On the other hand, below 440 K, the behavior of the LEED pattern is similar to the one observed in the NW case: the background intensity is getting brighter and the main substrate spots progressively lose intensity and disappear with increasing thicknesses. The satellite spots become more and more elongated, leaving concentric arcs [Fig. 3(d)].

In this temperature range, there is no significant variation (less then 0.5%) of the interlayer spacing with the thickness, as monitored by the specular *I(V)* LEED curves.

Two additional experiments were performed by evaporating Cr at room temperature on annealed or as grown Cr/Co(0001) interfaces. In the first experiment, 6 Å Cr was deposited at 300 K (in a NW orientation) and then annealed at about 500 K until a 1×1 hexagonal LEED pattern was obtained (the Cr Auger intensities were reduced after annealing). Further Cr deposition at room temperature led to the NW orientation. In the second experiment, about 6 Å Cr was evaporated on a substrate held above 440 K in order to obtain the KS orientation, and then, the sample was cooled down to room temperature. On further Cr deposition on this interface, the following Cr layers grow in a KS orientation, even for room-temperature growth. The interest of these last two experiments will become clear in the next section.

IV. DISCUSSION

In the case of bcc (110)/hcp (0001) or bcc (110)/fcc (111) interfaces, there are mainly two types of orientational relationships, NW or KS, as described above [Figs. 2(c) and 3(c)]. They both consist of a one-dimensional matching; i.e., there is only one direction in the epitaxial plane where the lattice parameters of the adsorbate and substrate are close together. From geometrical considerations, justified by energy calculations, it has been shown that the perfect NW orientation occurs when the fcc to bcc nearest-neighbor ratio r is $r_x=0.9428$ (NW_x) or $r_y=1.1547$ (NW_y). The perfect KS orientation is obtained for $r_k=1.0887$.[9,10] In the case of the Cr/Co interface, $r=1.004$. This value is just between r_x and r_k, placing that system in a limit case.

For growth temperature below 410 K, the NW structure is observed. Considering one domain [Fig. 2(c)], the lattice parameter along the [110] direction is expanded by about 6% with respect to bulk Cr, so that a nearly perfect matching with the Co[1230] direction is thus obtained (spacing between Co atoms in this row is 4.34 Å). On the other hand, there is no distortion of the Cr[001] direction. This 6% expansion allows a nearly perfect NW_x epitaxy, at least up to a thickness of several Cr layers. Taking these parameters of the in-plane cell, one should expect a Poisson contraction of about 2% in the direction perpendicular to the film plane. This is not observed, but bulk elastic considerations are not valid for the very surface or interface layers, because of the well-known surface relaxation phenomena. The failure of the elastic model has already been observed in similar systems

(see, e.g., Refs. 11 and 12). Because of this strong expansion, strain release occurs when the film is growing thicker. As a consequence, there must be formation of dislocations. The lattice parameter matching is thus getting poorer and the extension of the ordered domains is limited to several atomic rows along the [110] direction of Cr. Such elongated domains have been observed by scanning tunneling microscopy on the Fe/Au(111) system.[13] The limited extension in the [110] direction will lead to the elongated LEED spots in the corresponding direction as can be seen in Fig. 2(d). This discussion of course also holds for the other domain types. The streaks connecting the spots of two different types of domains indeed make an angle of 60°. There is no disorder in the other in-plane direction, since stress release is not needed. In the [110] direction, perpendicular to the film plane, there is also strain release as indicated by the *I(V)* curves. The bulk Cr interlayer spacing is obtained for thicknesses where the LEED diagrams show elongated spots as seen in Fig. 2(d). At this stage the Cr film is strain free (or nearly) in both perpendicular and parallel film plane directions.

Above 410 K a 1×1 structure is observed up to 3 Å film thickness. The structure turns to a KS orientation for higher thicknesses. The transition from the NW to the pseudomorphic-KS structure takes place at a temperature (about 410 K) where the Auger growth kinetics deviates from the simultaneous layers growth mode. However, the evolution with temperature of the growth kinetics is very progressive, much less abrupt than the one observed by LEED. As mentioned in Sec. III B, this behavior is compatible either with the progressive onset of a three-dimensional growth, or with a diffuse interface formation. Though there is no evidence of chemical shifts in the $2p$ and $3p$ Co and Cr core levels analyzed by XPS, several arguments support an alloying effect at the interface: first, at 470 K the low-energy Auger transitions of Co are still visible up to thicknesses of more than 50 Å, as well as the substrate spots in LEED. In the assumption of a three-dimensional island growth mode, in order to keep agreement with the Auger and LEED results, this would imply that there is grossly a full layer of Cr less than 5 Å thick on top of the Co substrate, and several hundred Å high Cr columns covering only half of the sample surface. Such a rough interface has not been observed in multilayers. The reflection high-energy electron diffraction diagrams obtained during multilayer growth clearly demonstrate smoother growth at elevated temperatures than at room temperature.[4] The NMR experiments in the same study indeed show that there is a diffuse Cr/Co interface when the growth is performed at 370 K (however, one has to be careful since NMR averages over two types of interfaces in the multilayers, Cr/Co and Co/Cr, which are *a priori* not equivalent).[4] Moreover, Cr has the low surface energy ($\gamma_{\mathrm{Cr}}=2.1\ \mathrm{J\,m^{-2}}$, $\gamma_{\mathrm{Co}}=2.7\ \mathrm{J\,m^{-2}}$), which does not favor a three-dimensional island growth. Though the Co-rich side of the phase diagram is still unknown and discussed, it seems that Co and Cr are miscible and that ordered hexagonal bulk alloys and solid solutions should be possible.[14,15] Thus, we think that between 400 and 440 K, a diffuse hexagonal Co-Cr interface first starts forming and then bcc Cr layers go on growing on top of it. It is, however, difficult to know experimentally if the pseudomorphical layer observed for a low thickness consists in a pure hexagonal Cr layer or is already a diffuse Cr-Co layer.

For a film thickness above 3 Å, the bcc layers are slightly strained since there is a slight expansion of about 1% in the bcc [110] direction. This corresponds actually to a 0.6% expansion of the spacing between the atoms along the [111] direction. As in the NW case, this expansion allows a perfect KS matching between the bcc [111] and hcp [1120] dense directions (the nearest-neighbor spacing of Cr and Co are then equal). Between 410 and 440 K, upon further Cr deposition, the competition between growing further Cr layers and alloying is still in favor of the growth. A strain release occurs with increasing film thickness. Here it is less clear how the strain release occurs. The above-mentioned 1% expansion results probably from a more complicated global distortion of the rectangular Cr cell, since it is also angular stressed. The concentric arcs in the LEED pattern of Fig. 3(d) can be explained in two ways: a relaxation of the 5.26° angle between the rectangular and hexagonal cells can produce angular disorder, which will lead to arcs in the LEED pattern; alternatively, a simple model of uniaxial disorder along the [111] direction (due to the formation of dislocations) shows streaks like those observed in the LEED pattern. Both explanations probably hold.

For temperatures higher than 440 K, the diffusion mechanism becomes more active, and there are only several bcc Cr layers remaining on top of a diffuse hexagonal interface. These layers are nearly strain free and do not get thick enough to show any relaxation.

In the following, we will try to discuss the possible origins of the structural transition from the NW structure below 410 K to the pseudomorphic-KS structures above 440 K. A rather similar behavior has been observed on Pd/Mo(110) for which $r=1.009$.[16] In this case a pseudomorphic growth followed by a NW orientation is obtained at room temperature and at 700 K there is a Pd-Mo alloy in a KS orientation on top of Mo(110).

From the work of Bauer and van der Merwe one can see (Fig. 4 in Ref. 9) that for certain values of the two parameters r and l there is a region in the phase diagram where pseudomorphism, NW, or KS orientations are equally probable. The parameter r has already been defined and is the nearest-neighbor-distance ratio between the fcc/hcp and bcc lattices and $l=\sqrt{\Omega S/r^2W}$, where W is the atomic volume of the adsorbate, S is a function of the stiffness coefficients, and W is a proportional to the adatoms' diffusion energy. Very tiny changes, either in r or l, due, e.g., to the growth of an alloyed interface, would be sufficient to explain the different crystallographic structures observed.

In order to test the influence of alloying, we prepared Cr/Co substrates as described in the last part of Sec. III. In the first experiment, by annealing Cr films on Co(0001) grown at room temperature we produce a hexagonal Co-Cr surface alloy. However, one can notice that it is not equivalent to grow a film at room temperature and then anneal it at a given temperature or to deposit it directly at the same temperature. If the consequence of alloying is either a surface parameter variation, or a change in the l factor, we should obtain the KS structure when Cr is deposited on this interface. This is actually not the case, since only the NW orientation is observed. On the other hand, the second experiment

shows that Cr layers keep on growing in the KS structure even at room temperature when deposited on a Cr/Co interface in the KS structure.

These two experiments demonstrate that alloying does not play the most important role in the structural transition, which is certainly related to temperature-driven kinetical effects. As is known from theoretical calculations and experimental systems,[17–22] the nucleation process is strongly temperature dependent. Different growth temperatures will lead to different island sizes. The height of the islands and their morphology, as well as the nucleation sites, may also change: at low temperature, the nucleation mainly occurs on defects (dislocations, step edges, kinks, reconstruction, etc.) whereas at higher temperatures the process is governed by the enhanced surface diffusion (see, e.g., Ref. 22). Thus, the epitaxial strain release will not occur in the same way for the different growth temperatures. In addition, surface defects play an important role in the misfit accommodation processes occurring, e.g., in the NW or KS structures.[23,24] An elastic calculation of the strain energy for a Cr cluster on top of Co(0001), using a simple Keating model,[25] shows that the epitaxial strain energies obtained for the experimentally observed NW and KS structures are very sensitive to the number of atoms in the cluster, of its height and even of the shape (particularly for clusters in the KS orientation). This calculation, however, does not take into account the strain release due to dislocation formation, or dynamical processes occurring during the growth, and is thus unable to give reliable structure predictions in our case.

This discussion may explain the different results obtained in other works. In the case of the pseudomorphical growth of Cr on Co/W(110),[5] the Co buffer is strongly distorted, even for a large Co thickness.[26] The surface cell no longer has a sixfold symmetry. There is one matching direction that is slightly favored, and thus only one domain orientation is observed. For the Co/Cr multilayers, both NW and KS orientations are observed simultaneously on the same sample.[4] This was never the case in our experiment, and we suggest the following explanation: the growth temperature of these multilayers is very close to the temperature where we observe the NW to KS transition. At this temperature the NW and KS structures should be nearly degenerated energetically and one should indeed observe both structures. However, a low deposition rate, as used in our case, favors the surface diffusion and the nucleation on surface defects. This process can lift up the degeneracy and thus only one type of structure is observed. On the other hand, in the case of multilayer growth the density of defects of the mica and GaAs substrates is expected to be very different from that of our single crystal, and the evaporation rate used is much higher. This will lead to a very different nucleation process, governed by the high deposition rate.

V. CONCLUSION

The growth of Cr on the Co(0001) surface strongly depends on the substrate temperature. Between 300 and 410 K there is no or limited interdiffusion and a simultaneous layer growth of Cr is observed. The layers are in a strained bcc (110) structure with a Nishiyama-Wassermann orientation. Above 410 K the interface is probably getting more and more diffuse with increasing temperature. A slightly strained (110) bcc Cr overlayer remains on top of the interface in a Kurdjumov-Sachs orientation. For a growth temperature below 440 K, the Cr films show strain release with increasing thickness, leading to uniaxial disorder as seen in the LEED pattern. The temperature-dependent growth mode and structure are tentatively ascribed to kinetical nucleation and surface diffusion processes leading to different film morphologies and thus to different ways of misfit accommodation.

ACKNOWLEDGMENTS

We are grateful to F. Sirotti for providing us with high purity Cr. We also express our thanks to M. C. Cadeville, B. Legrand, S. Andrieu, and H. Ardhuin for valuable discussions and to J. Hommet for his technical help.

[1] For a list of references see, for instance, N. Metoki, W. Donner, and H. Zabel, Phys. Rev. B **49**, 17 351 (1994).

[2] J. C. A. Huang, Y. Liou, Y. D. Yao, W. T. Yang, C. P. Chang, S. Y. Liao, and Y. M. Hu, Phys. Rev. B **52**, R13 110 (1995).

[3] W. Vavra, D. Barlett, S. Elagoz, C. Uher, and R. Clarke, Phys. Rev. B **47**, 5500 (1993).

[4] Y. Henry, C. Meny, A. Dinia, and P. Panissod, Phys. Rev. B **47**, 15 037 (1993).

[5] J. Kohlhepp, H. Fritzsche, H.-J. Elmers, and U. Gradmann, J. Magn. Magn. Mater. **148**, 95 (1995).

[6] D. Tian, F. Jona, and P. M. Marcus, Phys. Rev. B **45**, 11 216 (1992).

[7] M. P. Seah and W. A. Dench, Surf. Interface Anal. **1**, 2 (1979).

[8] C. Argile and G. E. Rhead, Surf. Sci. Rep. **10**, 280 (1989).

[9] E. Bauer and J. H. van der Merwe, Phys. Rev. B **33**, 3657 (1986), and references therein.

[10] M. Kato, Mater. Sci. Eng. **146**, 205 (1991).

[11] E. Snoek, S. Frechengues, M. J. Casanove, C. Roucau, and S. Andrieu, J. Cryst. Growth **167**, 143 (1996).

[12] C. Liu and D. Bader, Phys. Rev. B **41**, 553 (1990).

[13] B. Voigtländer, G. Meyer, and N. M. Hammer, Surf. Sci. **255**, L529 (1991).

[14] A. T. Grigorev, Yu-Pu Yeh, and E. M. Sokolovskaya, Russ. J. Inorg. Chem. **6**, 1827 (1961).

[15] E. Raharisoa, A. Dinia, P. Vennégues, and M. C. Cadeville (unpublished).

[16] Ch. Park, E. Bauer, and H. Poppa, Surf. Sci. **154**, 371 (1985).

[17] J. Jacobsen, K. W. Jacobsen, and J. K. Nørskov, Surf. Sci. **359**, 37 (1996).

[18] H. Brune, H. Röder, K. Bromann, K. Kern, J. Jacobsen, P. Stoltze, K. Jacobsen, and J. K. Nørskov, Surf. Sci. **349**, L115 (1996).

[19] M. C. Bartlett and J. W. Evans, Surf. Sci. **314**, L829 (1994).

[20] J. P. Bucher, in *Atomic and Molecular Wires*, edited by C. Joachim and S. Roth, Vol. 341 of NATO Advanced Studies

Institute Series E: Applied Sciences (Kluwer Academic, Dordrecht, 1997), p. 1.

[21] H. Röder, E. Hahn, H. Brune, J. P. Bucher, and K. Kern, Nature (London) **366**, 141 (1993).

[22] H. Gentner, F. Scheurer, T. Detzel, and J. P. Bucher, Thin Solid Films **275**, 58 (1996).

[23] G. J. Shiflet and J. H. van der Merwe, Metall. Mater. Trans. A **25A**, 1895 (1994).

[24] G. J. Shiflet and J. H. van der Merwe, Acta Metall. Mater. **42**, 1189 (1994); **42**, 1199 (1994).

[25] P. N. Keating, Phys. Rev. **145**, 637 (1966).

[26] H. Fritzsche, J. Kohlhepp, and U. Gradmann, Phys. Rev. B **51**, 15 933 (1995).